Stand-Alone Renewable Power System Scheduling for a Green Data-Center using Integer Linear Programming Version 1

Maroua Haddad, Jean-Marc Nicod, Marie-Cécile Pera, Christophe Varnier

INSTITUT FEMTO-ST

UMR CNRS 6174

Stand-Alone Renewable Power System Scheduling for a Green Data-Center using Integer Linear Programming

Version 1

Maroua Haddad, Jean-Marc Nicod, Marie-Cécile Péra and Christophe Varnier

Rapport de Recherche n° RR–FEMTO-ST–7927

DÉPARTEMENT AS2M – March 27, 2019

Stand-Alone Renewable Power System Scheduling for a Green Data-Center using Integer Linear Programming

Version 1

Maroua Haddad, Jean-Marc Nicod, Marie-Cécile Péra and Christophe Varnier

Département AS2M

PHM

Rapport de Recherche n° RR –FEMTO-ST–7927 March 27, 2019 (pages)

Abstract: Taking into account the spread of data centers around the world and their huge energy consumption, several researchers focused on task scheduling and resource allocation problem in order to minimize the energy consumed by the data center. Other initiatives focus on the implementation of green energy sources in order to minimize the consumption of fossil fuels and their emission of CO2. As part of the DATAZERO project, several teams are trying to define main concepts of a full green data center, only powered by renewable energies. To achieve this goal, it is necessary to focus on the efficient management of an autonomous hybrid power system consisting of solar panels, wind turbines, batteries and fuel cell systems. In this paper, we propose a model based on a mixed integer linear program to optimize the commitment of energy sources. The approach takes the season and weather forecasts into account at the time of optimization.

Key-words: Renewable energy, wind turbine, photo-voltaic panel, energy storage management, data center, integer linear program, optimization.

FEMTO-ST Institute, AS2M research department
TEMIS, 24 rue Alain Savary, F-25000 BESANÇON FRANCE
Tel: (33 3) 81 40 28 01 – Fax: (33 3) 81 40 28 09 – e-mail: isabelle.gabet@ens2m.fr

Optimisation de l'engagement des sources pour un Data Center approvisionné en énergie renouvelable

Version 1

Résumé : De nombreux chercheurs se sont intéressés récemment à la problématique de la sauvegarde d'énergie dans les datacenters. La plupart des travaux adresse les problèmes notamment d'ordonnancement et d'allocation de ressources pour minimiser l'énergie consommée par le data center. Quelques initiatives s'intéressent à la mise en œuvre de sources d'énergie verte afin de minimiser la consommation des énergies fossiles et leur émission de CO2.

Dans le cadre du projet de recherche DATAZERO, plusieurs équipes cherchent à définir les concepts d'un datacenter qui ne serait alimenté que par des énergies renouvelables. Il est alors nécessaire de s'intéresser à la gestion efficace d'un système d'alimentation hybride autonome composé de panneaux solaires, d'éoliennes, de batteries et de systèmes piles à combustible. Nous proposons dans cet article un modèle basé sur la programmation linéaire mixte pour optimiser l'engagement des sources d'énergie. L'approche tient compte de la localisation, de la saison et des prévisions météorologiques au moment de l'optimisation.

Mots-clés : Energie renouvelable, éolienne, panneau photovoltaïque, gestion du stockage d'énergie, centre de données, programme linéaire entier, optimisation

FEMTO-ST Institute, AS2M research department
TEMIS, 24 rue Alain Savary, F-25000 BESANÇON FRANCE
Tel: (33 3) 81 40 28 01 – Fax: (33 3) 81 40 28 09 – e-mail: isabelle.gabet@ens2m.fr

Stand-Alone Renewable Power System Scheduling for a Green Data-Center using Integer Linear Programming

Maroua Haddad, Jean-Marc Nicod, Marie-Cécile Péra and Christophe Varnier

March 27, 2019

Abstract

Taking into account the spread of data centers around the world and their huge energy consumption, several researchers focused on task scheduling and resource allocation problem in order to minimize the energy consumed by the data center. Other initiatives focus on the implementation of green energy sources in order to minimize the consumption of fossil fuels and their emission of CO2. As part of the DATAZERO project, several teams are trying to define main concepts of a full green data center, only powered by renewable energies. To achieve this goal, it is necessary to focus on the efficient management of an autonomous hybrid power system consisting of solar panels, wind turbines, batteries and fuel cell systems. In this paper, we propose a model based on a mixed integer linear program to optimize the commitment of energy sources. The approach takes the season and weather forecasts into account at the time of optimization.

1 Introduction

The enormous growth of the internet and the increase in the number of online services accessible to public have highlighted the cost imposed by the Cloud in general and by data centers in particular in terms of energy consumption over the past few years. Actually, a typical datacenter includes hundreds of thousands of servers, cooling equipment, and substation transformers which contribute hardly in global warming as they deliver a huge quantity of CO2.

In this context, many green initiatives are being taken to make the use of data centers more virtuous in terms of their ecological footprint. One of these initiatives is the use of renewable energy sources (RES) in data center power system and even make sure that energy production is directly integrated into their own facilities. Thus, McGraw-Hill companies recently completed a 14.1 MW solar panel installation to power its data center located in East Windsor [26]. Similarly, Apple has built a 40 MW solar field for its North Carolina data center [2]. Nevertheless, the intermittent nature of renewable energy sources (sun and wind) is driving these data centers to resell surplus energy and use conventional sources to provide continuous service. This economically viable energy policy is not entirely satisfying in terms of carbon footprint.

For this reason, the ANR DATAZERO project adopts an original approach which consists in computing data center's resources provisioned with 100% renewable energy. Designing and operating such a data center is however not trivial. There is a need to optimize the IT load to the energy availability, and conversely, to optimize the energy production to the incoming IT load. The sizing of the system in terms of IT and electrical components is also a huge challenge. Thus, the ANR DATAZERO project is divided on two main decision modules; an IT decision module (ITDM) responsible for the management of the IT part (scheduling tasks, virtualization of servers, etc.) and a power decision module (PDM) responsible for the management of the renewable sources (source commitment, storage, etc.). The project ambition consists in converging user needs with renewable energy production thanks to a negotiation loop (NM) [6] as explained in Figure 1. In fact, at each step of this negotiation, one asks to receive one or multiple energy profiles that could be delivered by the data center electrical part and needed to be consumed by the IT part to satisfy a given level of computation for final client. The negotiation will continue bargaining with the two modules till reaching the achieved convergence between the IT and electrical power profiles. So, depending on the circumstances and on the period of the year, the level of energy available for the calculations may vary. The principle is that the sizing of both the IT and the electrical parts must allow a computation service in accordance with the quality of service announced in full autonomy thanks to short and long-term storage devices. These storage devices help smooth the energy production available to the data center so that they can provide online services all day and all year long. However, the energy demand is not constant over time because client demand varies. Thus, minimizing the use of storage in view of a given calculation demand to satisfy, and therefore an electrical power to supply, is always the best solution. Therefore, in case of reduction of the energetic envelope, machines can be extinguished, virtual machines can be migrated, etc. Conversely, in the event of a strong demand from the servers, some of the energy can be drawn in addition to that coming directly from the wind turbines and / or solar panels. Here, long-term storage is done through the production of hydrogen with electrolyzers and the reverse generation of electricity is done with fuel cells [15].

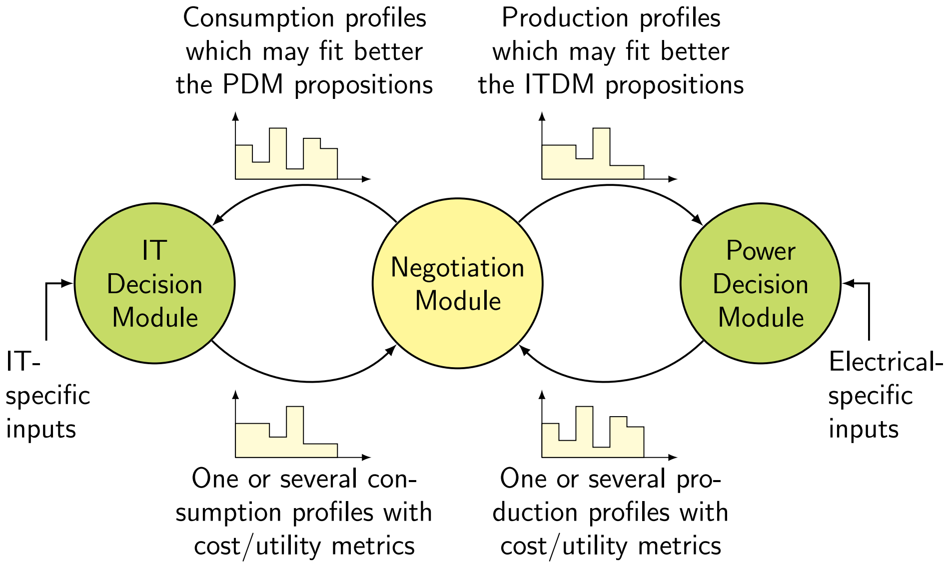

Figure 1: Illustration of the negotiation process, with the information exchanged between the decision modules and the negotiation module.

Thus, this article presents, as part of the ANR DATAZERO project, an efficient management of a hybrid renewable energy system (HRES) consisting of solar panels, wind turbines, batteries and fuel cell systems with electrolyzers to supply a data center without exchange with the external electricity network. Depending on the quantity of renewable energy produced over time, the storage sources must be managed. For instance, if the renewable production exceed the data center's demand, the energy difference should be stored. Conversely, in case the client demand is higher than the renewable production, the storage devices should provide the energy difference. Then, according to the negotiation setp, we propose here an electrical optimization steps consisting of three main objectives: (i) proposing which power profiles (constant or not) on a given period of time that the electrical part is able to produce to supply the IT part;(ii) proposing alternative power profiles based on a power profile given as an input by the negotiation module and (iii) proposing electrical power commitment in a given time window if we know the expected power demand of the data center that has to be satisfied; Only the power source commitment (i) is an input of the power system. The other optimization results that are power profile computed by (ii) and (iii) are sent to the negotiation module to help the negotiation process to converge. Once the convergence is obtained, the chosen power profile is delivered to the power decision module to compute the step (i) as mention before. The optimization is based on the optimal solving of Mixed Integer Linear Programs (MILP) as presented in the following.

The remainder of this paper is organized as the follows: Section 2 is dedicated to related works. In Section 3 we are proposing electrical component models on which constraints of the electrical part are based. The next section is focusing on the addressed problem within this paper. The Section 5 describes the linearization of the previous non-linear models. Additional constraints and three objective functions are also given in the section to define three MILPs, each of them corresponding to one problem (i), (ii) and (iii) described above. The Section 6 shows the usage of the Power Decision Module (PDM) that optimally solves addressed optimization problems. As a result of our approach, traces of executions are given to illustrate the PDM use in a time window of 72 hours on different periods of the year. The presented solutions are necessary optimal because of the use of MILP solved using Gurobi. Finally Section 7 gives a conclusion and perspectives.

2 related work

Taking into account climate change, oil depletion, increasing population and increasing energy demand, energy saving has become a major concern for the world in general and in the computing domain in particular. A large variety of research are working on reducing CO2 emissions and optimizing energy consumption. For instance, Oró *et al.* and Kaur *et al.* presented these surveys [28, 19] where they summarize all the technologies and tools that can be used in data centers to decrease their energy consumption.

Among many alternative energy sources, using green energy to power data centers can be considered as an attractive solution to succeed energy saving and reducing gaz emissions. For example, Microsoft's data center in Quincy, WA consumes 48 MW electricity which is enough to power 40,000 homes [18]. In Thibodaux, a city in Louisiana state planned a wind power data center project in urban area [31].

Following green peace report [5] of 2017, the consumption of data centers reached 7% of the world's energy, of which the half was dedicated to cooling [21]. Moreover, the AMD report [24] estimated that the electricity consumption of all data centers in the world costs 7.2 billion annually. Unfortunately, this consumption has a negative impact on the environment as the majority of electricity is produced from fossil resources. To further reduce the part of fossil fuels, many researchers were interested on the one hand in the management of energy resources to meet the demand of users, and on the other hand in the optimization of use of computing resources and networks to reduce overall energy consumption.

Managing energy sources in data centers. In this sense, Uddin *et al.* [35, 33, 32, 34] proposed also articles and surveys that tackle some strategies and techniques for energy efficiency and CO2 mitigation in data centers to lower the effect of global warming. A wide variety of research tackles the use of batteries in data centers [12, 11, 36, 37, 20]. These studies show that the use of the storage can lower both of the capital cost of the power delivery infrastructure and the operating cost of a data center. In addition, in almost all these papers, authors consider a workload with available grid power. Nevertheless, none of these works have taken into consideration the use of renewable energy sources. Then, many papers consider the coordination among multiple power sources in data centers. For instance, Arlit *et al* [3] introduce a management architecture that optimizes the combination of power grid usage and renewable energy sources (RES) from an economic point of view by balancing the demand for computing and resource availability with supply side constraints. In [7], Deng et al. have proposed online control policies that uses different characteristics of multiple power sources in order to minimize operation cost. These researchers use Lyapunov optimization and made a control algorithm which does not depend of statistics of system dynamics. Results show that it provide the trade-off capability between the operational cost, the data center availability, and the uninterruptible power supply (UPS) lifetime. The algorithms also achieve the robustness to time-varying power demand and supply. Another paper that also has considered the coordination among multiple power sources in green data centers is [23]. In this paper, Li et al. considered that data centers have base-load power supply, intermittent power supply, and backup energy storage. The authors argued that existing studies typically assume certain specific types of renewable energy sources, and overlook the benefits of cross-source coordination. Then, the authors have proposed a hierarchical power coordination scheme, taking into consideration the timing and capacity of different renewable energy sources. With this scheme, the data centers can make multi-objective power management decisions, based on the available base-load power output, renewable power variability, battery capacity, and IT jobs. Similarly, in [29] the source scheduling is based on a priority scheme in order to maximize the use of renewable energy. Thus the power consumption from the grid is minimized. A dynamic power technique is used to cap the energy used from the grid. In [8], Goiri *et al.* developed a prototype of an ecological data center connected to the grid in a small container including a set of solar panels, an electric battery and inverters. In their management algorithm, the authors take into consideration the electricity consumption and its cost. The results shows that this algorithm can produce integrated workload and energy source schedules for a low electricity costs.

Managing workloads in data centers. At the same time, work is being done to optimize IT resources in two directions. The first concerns the possibility to address the problem of scheduling computation tasks under energetic constraints [17, 22], problems of allocation and resource management with server shutdown, migration of virtual machines, etc. [4, 10, 30]. The other direction consists in imagining new architectures based on the use of ever greener energy [14, 16, 27].

An early work on green energy utilization in data centers by Aksanli et al. [1] shows the importance of power prediction. The authors designed an adaptive data center job scheduler capable of reducing the number of aborted jobs and improving the green energy utilization. In [9, 10], the authors propose GreenSlot which is a batch scheduler for parallel tasks. The aim is to reduce the brown power consumption of a data center partially powered by solar panels. In GreenSlot computation jobs have deadlines and the scheduler first reserves resources for these jobs with lower slack (distance from latest possible start time to current time). Based on weather forecasting and power prediction, GreenSlot schedules the tasks on time slots. However the authors do not try to optimize their schedules. They just reduce the consumption and costs while meeting as much deadlines as possible. Similarly [25] presents an holistic approach to optimize the energy cost with incomes from running a batch of jobs and outcomes to buy brown energy. The paper also provides a proposition for net zero scheduling batch of jobs. It is however based on virtualization and is not bounded by the number of resources.

None of the aforementioned work deals with computing resources provisioned with 100% renewable energy that we consider in this paper. The DATAZERO project then aims at conceiving an innovative structure of a datacenter where the IT module is explained in these articles [30, 4] Then, the management of the renewable energy sources of the power decision module is explained in this paper.

3 Model

As mentioned before, the power supply system of the data center consists of a photo-voltaic panels, a wind farm, an energy storage system (ESS) made of a battery bank, regenerative hydrogen energy units composed of proton exchange membrane fuel cell systems (PEMFC) combined with power exchange membrane electrolyzer units to supply the data center as shown in Figure 2. This hybrid system works as follows:

- Solar panels (photo-voltaic panels – PV) and wind turbines (WT) constitute the primary sources to supply the data center. In this paper, we consider the sources as a set independently of their quantity.

- Batteries and hydrogen system are the secondary sources, working as storage elements respectively for short term (within a day) and long term (seasonal) storage. In this paper, we consider the sources as a set independently of their quantity.

Moreover, to ensure the sustainability of the data center, the storage level of hydrogen must follow a predefined level ($LOHtarget_D$) for each day of a year. We assume that the target is known. It can be obtained thanks to a sizing and weather trend studies depending on the location of the data center. This study constitutes a challenging issue that is not addressed in this paper but included in the ANR DATAZERO project.

In order to properly analyze and implement this hybrid system, it is mandatory to describe the model of each component. For that, Table **??** and Table **??** lists all the notations used in the following sections. First of all, let $\mathcal{H} = K\Delta T$ a time window discretized into K identical periods of duration ΔT unit of time.

Depending on the case, let k defined as both the kth time step at instant $k\Delta T$ from the beginning of $\mathcal{H}$ and the index of the kth period ΔT of $\mathcal{H}$ defined between the two time step k and $k+1$ ($k \in [\![0, K]\!]$), *i.e.*, $k = K$ designs the first time step of the next time window.

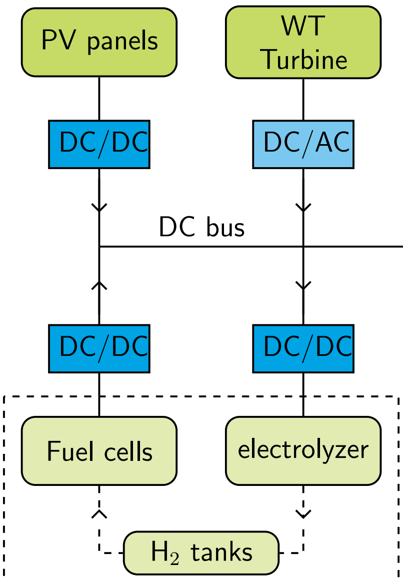

Figure 2: Structure of the DC microgrid supplying the datacenter loads.

Table 1: Nomenclature (1/2)

Variable	Description
Notations: Indices	
$\mathcal{H}$	a given time window
ΔT	interval of time between two time steps
k	index for one time step within $\mathcal{H}$
K	number of time steps within $\mathcal{H}$
Notations: Solar panel	
A_{pv}	PV area $[m^2]$
η_{pv}	PV efficiency [%]
I_k	Solar irradiation of tilted surface $[kW.m^{-2}]$
Ppv_k	PV power $[kW]$
Notations: Wind turbines	
A_{wt}	WT rotor swept area $[m^2]$
η_{wt}	WT efficiency[%]
Pw_k	Wind power $[kW]$
Pwt_k	WT power $[kW]$
Notations: Batteries	
$SOCmax$	State of Charge (SOC) upper limit $[kWh]$
$SOCmin$	SOC lower limit $[kWh]$
η_{ch}	Battery charge efficiency [%]
η_{dch}	Battery discharge efficiency [%]
σ	Battery self-discharge rate [%]
SOC_k	SOC at instant $k\Delta t$ $[kWh]$
Pch_k	Power used to recharge battery $[kW]$
$Pdch_k$	Power discharged from battery $[kW]$
Notations: Hydrogen tank	
$LOHtarget_D$	H_2 tank level targeted for a given day D
$LOHmax$	H_2 tank upper limit [%]
$LHVh_2$	H_2 lower heating value $[kWh.kg^{-1}]$
$HHVh_2$	H_2 higher heating value $[kWh.kg^{-1}]$
η_{tank}	H_2 tank efficiency[%]
LOH_k	H_2 tank inventory level $[kg]$
Notations: Electrolyzer	
$Pezmax$	Electrolyzer power upper limit [%]
$Pezmin$	Electrolyzer power lower limit [%]
η_{ez}	Electrolyzer efficiency [%]
Pez_k	Power put into electrolyzer $[kW]$
Qez_k	Electrolyzer H_2 mass flow $[kg]$

3.1 Component models

- **Photovoltaic panels**: The relation between the irradiation data I_k at time step k, the area of the PV panels A_{pv}, PV panels efficiency η_{pv} and the output power Ppv_k of the PV panels is described in Equation (1):

$$Ppv_k = I_k \times A_{pv} \times \eta_{pv} \tag{1}$$

Table 2: Nomenclature (2/2)

Variable	**Description**
	Notations: Fuel Cell
$Pfcmin$	Minimum power to operate fuel cell $[kW]$
$Pfcmax$	Maximum power delivered by fuel cell $[kW]$
η_{fc}	Fuel Cell efficiency [%]
Pfc_k	Power delivered by fuel cell at period k $[kW]$
Qfc_k	Fuel cell H_2 mass flow $[kg]$
	Notations: other
η_{inv}	Inverter efficiency [%]
x_k	Battery in use ($x_k = 1$) or not ($x_k = 0$)
y_k	Electrolyzer in use ($y_k = 1$) or not ($y_k = 0$)

- **Wind turbines**: The total power output Pwt_k of the wind turbine generator at a time step k in function of the total swept area by the blades A_{wt} and the efficiency of the wind turbine η_{wt} is given by Equation (2):

$$Pwt_k = Pw_k \times A_{wt} \times \eta_{wt} \tag{2}$$

where Pw_k follows the mathematical model (3) in function of the wind speed values:

$$Pw_k = \begin{cases} 0 & \text{if} \quad v(k) \leq v_{ci} \text{ or } v(k) \geq v_{co} \\ P_r \dfrac{v^3(k) - v_{ci}^3}{v_r^3 - v_{ci}^3} & \text{if} \quad v_{ci} < v(k) < v_r \\ P_r & \text{if} \quad v_r < v(k) < v_{co} \end{cases} \tag{3}$$

where v in the wind speed, v_{ci} is the cut in wind speed for which the wind turbine start working, v_{co} is the cut out wind speed for which the wind turbine stops working, v_r is the rated wind speed for which the wind turbine operate in its rated power P_r

- **Batteries**: The charging and discharging equations of a battery are calculated for each k with $k \in [\![1, K]\!]$ respectively in Equations (5) and (6) and with respect to the previous state of charge of the battery SOC_{k-1}, the self-discharge rate σ, the charging, discharging power Pch_{k-1}, $Pdch_{k-1}$ and the charging, discharging efficiency η_{ch}, η_{dch}:

$$\begin{aligned} SOC_k = {} & SOC_{k-1} \times (1 - \sigma) + Pch_{k-1} \times \eta_{ch} \times \Delta t \\ & - \frac{Pdch_{k-1}}{\eta_{dch}} \times \Delta t \\ & \text{with} \quad SOCmin \leq SOC_k \leq SOCmax \end{aligned} \tag{4}$$

where the charging and discharging process is limited by the battery capacity:

$$\begin{aligned} SOC_k = \min\{ & SOC_{k-1} \times (1 - \sigma) + Pch_{k-1} \\ & \times \eta_{ch} \times \Delta t, SOCmax\} \text{ if } Pch_{k-1} > 0 \end{aligned} \tag{5}$$

$$SOC_k = \max\{SOC_{k-1} \times (1 - \sigma) - \frac{Pdch_{k-1}}{\eta_{dch}} \tag{6}$$

$$\times \Delta t, SOCmin\} \text{ if } Pdch_{k-1} > 0$$

The battery energy system (BES) cannot charge and discharge at the same time. In fact, the charging process ends when either the BES system reaches the maximum capacity or the available energy that has to be stored is charged with on the BES. On the contrary, if the energy production cannot satisfy the energy demand, the battery starts the discharging process until the lower capacity limit is reached or the load demand is completely met.

- **Electrolyzer**: The H_2 mass flow Qez_k produced depends on the operating power Pez_k of the electrolyzer. The following relations is defined for each period k ($k \in [\![0, K-1]\!]$):

$$Pez_k \times \Delta t = \frac{HHVh_2 \times Qez_k}{\eta_{ez}} \quad (7)$$
$$with \quad Pezmin \leq Pez_k \leq Pezmax$$

with $Pezmin$, $Pezmax$ the operating range of the electrolyzer, Qez_k the electrolyzer H_2 mass flow (kg), η_{ez} the efficiency of the electrolyzer and $HHVh_2$ hydrogen higher heating value.

- **Fuel Cell**: The output power of the fuel cell Pfc_k is calculated at any time during each period k ($k \in [\![0, K-1]\!]$) following Equation (8):

$$Pfc_k \times \Delta t = LHVh_2 \times Qfc_k \times \eta_{fc} \quad (8)$$
$$with \quad Pfc_k \leq Pfcmax$$

with Qfc_k the H_2 mass flow (kg) passing by the fuel cell, η_{fc} the efficiency and $LHVh_2$ the low heating value of hydrogen.

- **Hydrogen tank**: The hydrogen produced by the electrolyzer and consumed by the fuel cell is stored in tanks. Thus, The level of hydrogen in the tank is calculated at any time during each period k with $k \in [\![1, K]\!]$ as follows, with η_{tank} the efficiency related to the hydrogen relaxation:

$$LOH_k = LOH_{k-1} + Qez_{k-1} - Qfc_{k-1} \quad (9)$$
$$\text{with } 0 \leq LOH_k \leq LOHmax \quad (10)$$

where LOH_0 is the initial value of the level of hydrogen

Considering the previous simplified model for all energy sources, we propose to show how they can be used to solve optimization problems we faced.

4 Problem statement

The negotiation module aims to guide both the decision optimization modules ITDM and PDM in order to converge to a power profile, first, close to the one requested by IT and second, feasible by the electrical part. In evidence, the IT decision module would prefer to execute jobs when that is better for QoS constraints. However, it most likely may not match with the best usage of renewable energy and storage devices. Then, it is mandatory to confront IT requests with the energy availability which is computed by the PDM. As a consequence, the strategy

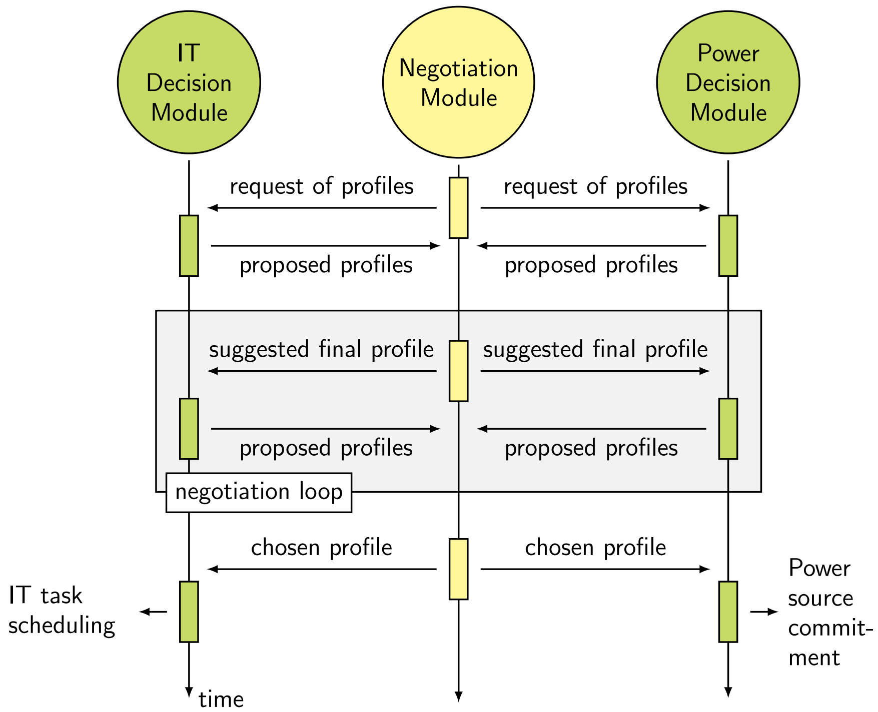

Figure 3: Illustration of the negotiation process, with the information exchanged between the decision modules and the negotiation module.

describing the exchange of power profiles between the three modules is done as illustrated in Figure 3 and will be explained in details in the next subsection.

Thus, the negotiation module forces both ITDM and PDM to design one or multiple power profiles and to send them for each negotiation round. In order to converge and to find the best commitment for both modules, the power profile sent must be different of the one sent before in the previous round of negotiation. Therefore, the power decision module addresses different optimization problems according to the purpose of the work and the constraints of the system. The primary goal of the power management system consists in defining the best commitment to satisfy the power demand. Let one consider $\mathcal{H}$, ΔT, K and k as defined in the previous section. To make the optimization process readable, a list of the notations used is summarized within Table 1 and Table 2.

4.1 strategies of the power decision module

As seen previously in the negotiation process several kind of requests are asked to the power management module. This leads to design different kind of power profiles depending on the round of negotiation. Then, we can define multiple optimization program which address underlying problems. In the strategy proposed (see 3),the negotiation module (NM) starts by requesting different power profiles. PDM have to identify which source commitment can be proposed regarding the energy storage levels and the weather forecasting. This is done following two different goals:

- Providing the maximum constant power profile while respecting all the constraints and the storage state and taking into account the weather forecasting during the current horizon;

- Providing a non constant power profile where the goal consists in minimizing the loss due to the efficiency of the power sources while respecting all the constraints and the storage state.

In the second round of the negotiation, the NM send a power profile and asks to design a new profile that is close to the given one. In this case, the optimized program has another goal:

- Matching with the given load profile. The problem consists in maximizing the overall power production. Additional constraints force the power production for each period to be within an interval of values set by the suggested power profile sent by the NM, while respecting the constraints defined by the model and the storage state.

Once the negotiation ends, the NM send the chosen profile to both PDM and ITDM. Then, PDM has to find the best commitment of the power sources to answer to that chosen profile. This third problem follows another goal:

- Satisfying the load demand. The strategy proposed is to maximize the long-term storage by setting a target level to reach at the end of the horizon. This allows to ensure the seasonality variation of renewable energy production.

All the previously described strategies are based on common constraints that translate the physical laws of the power system. The remainder of this section describes those constraints.

4.2 Flow conservation

The energy produced ($Pwt_k + Ppv_k$) by the primary sources during the whole period k is used for three purposes:

- Hydrogen production (Pez_k)
- Charging the batteries (Pch_k)
- Satisfaction of the data center demand ($Pload_k$)

In case there is not enough renewable energy to meet the demand ($Pload_k$), additional electrical power is delivered by the fuel cells (Pfc_k) and batteries ($Pdch_k$). To satisfy the demand, Equation (11) should be fulfilled for each k with $k \in [\![0, K-1]\!]$:

$$\begin{aligned} Pload_k \leq\ & Pwt_k + Ppv_k + \\ & (Pfc_k + Pdch_k - Pez_k - Pch_k) \times \eta_{inv} \end{aligned} \tag{11}$$

4.3 Constraint Satisfaction Problem

The resulting model can be viewed as a Constraint Satisfaction Problem (CSP). In a second step, this model will be linearized in the next section to be solved using an efficient solver as Gurobi [13]. This allows to propose solutions optimally computed by the Power module of the project: (i) identification of the profile that maximizes the power produced, (ii) computation of an optimal commitment around a target profile considering a given relax factor, and (iii) computation of an optimal commitment constrained by the load profile.

As a result, the CSP is defined as follows (with $k \in [\![0, K-1]\!]$ or $k \in [\![0, K]\!]$ for SOC_k and LOH_k variables):

$$\begin{array}{l} Pload_k \leq Pwt_k + Ppv_k + (Pfc_k + Pdch_k) \\ \qquad\quad \eta_{inv} - (Pez_k + Pch_k)\eta_{inv} \\ \\ SOC_k = \min\{SOC_{k-1} \times (1-\sigma) + Pch_{k-1} \\ \qquad\quad \times\eta_{ch} \times \Delta t, SOCmax\} \quad \text{if } Pch_{k-1} > 0 \\ \\ SOC_k = \max\{SOC_{k-1} \times (1-\sigma) - \frac{Pdch_{k-1}}{\eta_{dch}} \\ \qquad\quad \times\Delta t, SOCmin\} \text{ if } Pdch_{k-1} > 0 \\ \\ Pez_k\Delta t = HHVh_2 \times Qez_k/\eta_{ez} \\ \\ Pfc_k\Delta t = LHVh_2 \times Qfc_k \times \eta_{fc} \\ \\ LOH_k = LOH_{k-1} + Qez_{k-1} - Qfc_{k-1}/\eta_{tank} \\ \text{Bounds:} \\ Pfc_k \leq Pfcmax \\ Pezmin \leq Pez_k \leq Pezmax \\ SOCmin \leq SOC_k \leq SOCmax \\ 0 \leq LOH_k \leq LOHmax \end{array} \tag{12}$$

4.4 Context of the resolution

In addition, common sense rules have to be considered to allow the use of power components without any time restriction if the two following constraints are respected:

- When a FC starts working, it is only used to satisfy the demand and not to charge batteries.
- When batteries start discharging, they are only used to satisfy the demand and not to produce hydrogen.

In the next section, we propose to transform the CSP in a linear constraint satisfaction problem.

5 Constraint Linearization

In this section, in order to be solved, the proposed CSP (12) is linearized.

5.1 Linearization of the constraints

Each constraint of the model is transformed to obtain a linear relation.

5.1.1 The battery state of charge

The state of charge of the battery is limited by the SOC range ($SOCmin$ and $SOCmax$) with $k \in [\![0, K]\!]$ and depends both on the charge and discharge phases:

$$\begin{cases} SOCmin & \leq SOC_k \leq SOCmax \\ SOC_k & = SOC_{k-1}(1-\sigma) + Pch_{k-1}\Delta t \times \eta_{ch} \\ & -Pdch_{k-1}\Delta t/\eta_{dch} \end{cases} \tag{13}$$

Because the both charge and discharge phases are concurrent phases, we introduce the set of binary variables x_k, and two sets of variables Pch'_k, $Pdch'_k$ and we propose to rewrite the previous state of charge equations as the following:

$$\begin{cases} SOCmin & \leq SOC_k \leq SOCmax \\ SOC_k & = SOC_{k-1}(1-\sigma) + x_k \times Pch'_{k-1} \times \\ & \Delta t \times \eta_{ch} - (1-x_k) \times Pdch'_{k-1} \Delta t / \eta_{dch} \end{cases} \tag{14}$$

where $x_k = 0$ means that the battery is discharging and $x_k = 1$ means that the battery is charging. In this way, the battery can not charge and discharge at the same time. Here, variable substitutions are also needed when introducing the set of variables Pch'_k and $Pdch'$ with $k \in [\![0, K-1]\!]$:

$$\begin{cases} Pch_k & = x_k \times Pch'_k \\ Pdch_k & = (1-x_k) \times Pdch'_k \end{cases} \tag{15}$$

Due to these substitutions, we add new constraints to linearize (14):

$$\begin{cases} 0 \leq Pch_k \leq Pchmax \\ Pch_k \geq 0 \\ Pch_k \leq x_k Pchmax \\ Pch_k \leq Pch'_k \\ Pch_k \geq Pch'_k - (1-x_k) Pchmax \end{cases} \tag{16}$$

$$\begin{cases} 0 \leq Pdch_k \leq Pdchmax \\ Pdch_k \geq 0 \\ Pdch_k \leq (1-x_k) Pdchmax \\ Pdch_k \leq Pdch'_k \\ Pdch_k \geq Pdch'_k - x_k Pdchmax \end{cases} \tag{17}$$

Because Equation (15) is not written within the final linear program, the fact that the battery can not charge and discharge is introduced by other new equations:

$$\begin{cases} Pch_k \leq x_k \times Pchmax \quad \text{with} \quad k \in [\![0, K-1]\!] \\ Pdch_k \leq (1-x_k) \times Pdchmax \quad \text{with} \quad k \in [\![0, K-1]\!] \\ x_k \in \{0, 1\} \end{cases} \tag{18}$$

where $Pchmax$ and $Pdchmax$ are the respective upperbound of Pch_k and $Pdch_k$.

Battery operation: The battery is supposed to balance underproduction and overproduction during a period of time T. For instance if $T = 24h$ with $\Delta t = 1h$ and $K = 24$, batteries are used for the fluctuations between day and night. It means that the production is smoothed over the day. To make it possible, the level of the state of charge of the battery should be greater or equal than its value at the beginning of each period T. This operation is explained by the following to fix values before the resolution of the program if T is larger than $24h$:

$$\begin{cases} SOC_K & = SOC_0 = SOCinit \text{ if } K < 24 \\ SOC_k & = SOC_0 = SOCinit \text{ if } K \geq 24 \\ & \text{and } k\%24 = 0 \ (k \in [\![0, K]\!]) \end{cases} \tag{19}$$

with $SOCinit$ the right level of charge to make possible the daily power compensation from hours where an extra renewable production is existing to hours this production is lacking. That is why this level has to come back to the same level each day. The difference between days is compensated by using long term storage.

5.1.2 Electrolyzer

When the electrolyzer operates, it must respect the power range, otherwise it will not work and its power will be equal to zero. The following bounds express these cases:

$$\begin{cases} \forall k \in [\![0, K-1]\!] & Pezmin \leq Pez_k \leq Pezmax \\ \forall k \in [\![0, K-1]\!] & Pez_k \geq 0 \end{cases} \tag{20}$$

It is then necessary to introduce a set of binary variables y_k to model the two alternatives where (with $k \in [\![0, K-1]\!]$):

- $y_k = 1$ means that the electrolyzer is in use with $Pezmin \leq Pez_k \leq Pezmax$ during period k;
- $y_k = 0$ means that the electrolyzer is stopped during period k.

$$\begin{cases} (1 - y_k) \times Pez_k = 0 \\ y_k \times Pez_k \leq Pezmax \\ y_k \times Pez_k \geq y_k \times Pezmin \\ y_k \in \{0, 1\} \end{cases} \tag{21}$$

Due to the non linearity of the set of equations (21), we propose to add a new set of variables y_k (with $k \in [\![0, K-1]\!]$) and variable substitutions to remain Pez_k to be the relevant variables that express the use of the electrolyzer. We define the following relation to make the linearization possible:

$$Pez_k = y_k \times Pez'_k \tag{22}$$

then we add the following equations to linearize (21):

$$\begin{cases} Pez_k \leq Pez'_k \\ Pez_k \geq 0 \\ Pez_k \leq y_k \times Pezmax \\ Pez_k \geq Pez'_k - (1 - y_k)Pezmax \\ 0 \leq Pez'_k \leq Pezmax \\ Pez_k \geq y_k \times Pezmin \\ y_k \in \{0, 1\} \end{cases} \tag{23}$$

5.1.3 Hydrogen tank level

As mentioned before for the battery, it is necessary to manage Qfc_k and Qez_k in order to control the hydrogen mass flow circulating in the hydrogen tank as mentioned in Equation (9).

Equations (7), (8) and (9) can be written by considering the new definition of Qez_k and Qfc_k for $k \in [\![0, K]\!]$:

$$\begin{cases} Pez_k \Delta t = HHVh_2 \times Qez_k / \eta_{ez} \\ Pfc_k \Delta t = LHVh_2 \times Qfc_k \times \eta_{fc} \\ LOH_k = LOH_{k-1} + Qez_{k-1} - Qfc_{k-1} / \eta_{tank} \end{cases} \quad (24)$$

Therefore, additionally to the two new sets of variables Qez'_k and Qfc'_k, we introduce an other set of binary variables z_k to model the two alternatives where the fuel cells are in use or not (with $k \in [\![0, K-1]\!]$). As before and for the same reasons, let be the following variable substitutions:

$$\begin{cases} Qez_k = z_k \times Qez'_k \\ Qfc_k = (1 - z_k) \times Qfc'_k \end{cases} \quad (25)$$

where:

- $z_k = 1$ means that $Qez_k = 0$
- $z_k = 0$ means that $Qfc_k = 0$

then we add the following set of equations :

$$\begin{cases} Qez_k \leq Qez'_k \\ Qez_k \geq 0 \\ Qez_k \leq z_k Qezmax \\ Qez_k \geq Qez'_k - (1 - z_k) Qezmax \\ 0 \leq Qez_k \leq Qezmax \end{cases} \quad (26)$$

$$\begin{cases} Qfc_k \leq Qfc'_k \\ Qfc_k \geq 0 \\ Qfc_k \leq (1 - z_k) \times Qfcmax \\ Qfc_k \geq Qfc'_k - z_k \times Qfcmax \\ 0 \leq Qfc_k \leq Qfcmax \end{cases} \quad (27)$$

In the rest of the document, we use these constraints as a basic model for the different applications of the PDM.

5.2 Additional linear constraints

As indicated in Section 4.4, let us recall the common sense usage rules.

5.2.1 Mutual exclusion between hydrogen and battery

The valid usage cases are:

1. The battery is in charge ($x_k = 1$) while electrolyzer can be in use ($y_k = 0$ or 1) and obviously fuel cell is stopped ($z_k = 0$).

2. The battery is discharging ($x_k = 0$) then fuel cell can be in use ($z_k = 0$ or 1) and the electrolyzer has to be stopped ($y_k = 0$).

3. The electrolyzer is in use ($y_k = 1$) with the battery in charge or not ($x_k = 0$ or 1), then the fuel cell is stopped ($z_k = 0$).

4. Start and stop of the fuel cell and the electrolyzer are allowed in this problem.

The following constraints represent the solution to these requirements:

$$\begin{cases} (1 - x_k) \times y_k = 0 \\ x_k \times y_k = y_k + x_k \times z_k \end{cases} \tag{28}$$

Due to the non linearity of the set of equations (28), we propose to add a new set of variables u_k and v_k (with $k \in [\![0, K-1]\!]$) that express the mutual exclusion between hydrogen and battery where:

- $u_k = x_k \times y_k$
- $v_k = x_k \times z_k$

then we add the following set of equations :

$$\begin{cases} u_k \leq x_k \\ u_k \leq y_k \\ 1 - x_k - y_k + u \geq 0 \\ u_k \geq 0 \end{cases} \tag{29}$$

$$\begin{cases} v_k \leq x_k \\ v_k \leq z_k \\ 1 - x_k - z_k + v \geq 0 \\ v_k \geq 0 \end{cases} \tag{30}$$

The obtained mixed integer linear program will be used in the following section as a basic model for the different optimization programs designed for the power decision module.

6 Power Decision Module PDM

In this section, the power decision module is the solver of the optimization problems that will be explained below according to the negotiation state. These optimization problems are solved using linear programming which is defined by a set of equations: an objective function and some constraints. Following the stage of the negotiation, the PDM should be able to provide the good commitment of the power sources. Thus, as detailed in section 4.1, the PDM is able to design different profiles in function of the goal it has to ensure.

The problem takes as input the renewable power produced under weather conditions $Prenew_k = Ppv_k + Pwt_k$, power demand $Pload_k$ and other information of sizing like number of wind turbine, pv panels, energy storage capacity and efficiency of any component, and generates a schedule of each time slot for supply-side source and energy storage usage, according to the availability of renewable power as explained in Section 3.1.

The optimization problems explained in the following paragraphs are programmed under python and solved using GUROBI solver [13]. The same sizing and the same weather conditions are applied to all the programs for a better illustration of the difference of results.

6.1 Providing a constant power profile *Pprod*

In this section, the aim is to obtain a maximum power production $Pprod$ from the primary sources for the whole horizon $\mathcal{H}$, taking into account the efficiency of each storage part used. Then the PDM will take as input the meteorological data to determine the primary production, the storage situation and the target set. As an output, the PDM must send the maximum constant profile and the storage situation to the negotiation module.

To make this possible, some modifications will be set for the mixed integer linear program and a new objective function and new constraints are added. To simplify it, the new variables added are explained in Table 3.

Table 3: Notations

Variable	**Description**
$Pprod$	The constant power profile $[kW]$
$LOHtarget_p$	A level of hydrogen defined by the sizing needed to be reached at the end of the horizon H $[kg]$

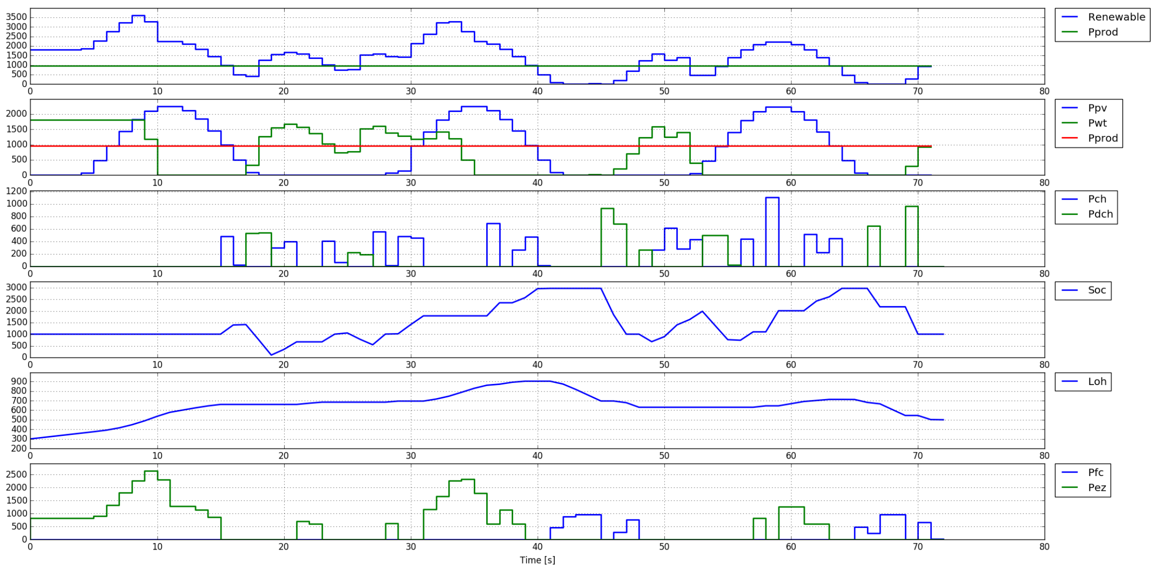

Figure 4: Constant Power Profile management

6.1.1 Objective function

The objective function consists of maximizing the constant power profile obtained from the source commitment $Pprod$ in order to propose a profile in the first part to the negotiation. The problem is thus mathematically translated to:

$$\text{maximize} \quad Pprod \tag{31}$$

6.1.2 Additional constraints

Some constraints are added or modified in order to consider common sense usage rules: consequently, Equation (11) is modified in this program as (32). Another constraint (33) is added to ensure the hydrogen level at the end of the period of simulation reached the target defined. This allows the storage system to handle the next periods.

$$\begin{aligned}\forall k \in [\![0, K-1]\!] \\ Pprod \leq & Pwt_k + Ppv_k + \\ & (Pfc_k + Pdch_k - Pez_k - Pch_k)\eta_{inv}\end{aligned} \tag{32}$$

$$LOHtarget_D \leq LOH_K \tag{33}$$

The hydrogen target level $LOHtarget_D$ is supposed to be computed based on long term weather forecasting and IT load consumption for one year. D represents the day number within the current year and matches with the time horizon $K \times \Delta t$.

6.1.3 Obtained model

The constraints explained in Section 5.1 are used for each version of the PDM as the basic constraints. Then, the linear program able to produce a constant maximum profile using the storage system composed of batteries and hydrogen system is then written as mentioned in the appendix B.

6.1.4 Results

In this linear program, we suppose that we are in the first stage of the negotiation which explains the absence of load in Figure 4. Actually, in that step of the negotiation, the PDM is supposed to provide the negotiation with profiles without getting data about the load. The same power architecture as in the previous section is used.

Results presented in Figure 4 are obtained by applying this linear program. The solution gives here a maximum constant power that can be delivered equals to 1 MW. As can be seen in the figure, the battery is responsible of the daily smoothing (day/night alternation). Thanks to the constraint (33), the level of hydrogen is even more than target at the end of the horizon $\mathcal{H}$ ($LOHtarget_D = 300\,kg$) to be able to assist the next horizon.

6.2 Providing a non constant power profile

In this section, the aim is to obtain a non constant power production profile $Pprod_k$ ($k \in [\![0, K-1]\!]$) from the primary sources, taking into account the efficiency of each storage part used. Then the PDM takes the meteorological data as an input to determine the primary production, the storage levels, etc., along the horizon $\mathcal{H}$.

As an output, the PDM must send the maximum power profile, and the storage situation to the negotiation module.

To make this possible, some modifications are set to the linear program obtained in the previous section. To simplify it, the variable $Pprod$ is no longer equal to a constant value during the horizon $\mathcal{H}$ but is changes following each step k in the horizon.

6.2.1 Objective function

For this strategy, the objective function consists of maximizing the power profile obtained from the source commitment *Pprod* in order to address to the data center load. The problem is thus mathematically translated to:

$$\text{maximize} \quad \sum_{k=0}^{K-1} Pprod_k \tag{34}$$

6.2.2 Added constraints

As in the constant power case, some constraints are added or modified to consider common sense usage rules then Equation (11) is modified in this program as (35):

$$\begin{aligned} &\forall k \in [\![0, K-1]\!] \\ &\quad Pprod_k \leq Pwt_k + Ppv_k + \\ &\qquad\qquad (Pfc_k + Pdch_k - Pez_k + Pch_k)\eta_{inv} \end{aligned} \tag{35}$$

The same constraint (33) is added to ensure the target level of hydrogen is reached at the end of the period of simulation, so that the storage system is able to handle the next periods.

In order to satisfy a minimum production to operate the data center, a new constraint is added to the linear program as defined in Equation (36):

$$Pprod_k \geq Pprodmin \tag{36}$$

Thus, the power produced in each time step k by the different sources should be greater or equal to the minimal production $Pprodmin = 1MW$.

6.2.3 Obtained model

The linear program is able to produce a maximum non constant profile using the storage system composed of batteries and hydrogen system is then written as in the appendix C

6.2.4 Results

Results presented in Figure 5 are obtained by applying this linear program. The production *Pprod* is variable in some time step k and greater than the minimal production *Pprodmin* (see for example at $t = 60$ h). The same power architecture is used as in the previous subsections. The minimal production is equal to $1MW$ in order to make the variations of *Pprod* more noticeable. The batteries assure the smoothing as in the last linear program and the level of the battery comes back to the intended one. The level of hydrogen at the end of the horizon is greater than the hydrogen level target fixed, then, the constraint (33) is respected.

6.3 Matching with a requested profile

In this subsection, the aim is to obtain a profile which is matching with a profile requested by the negotiation module to end up with the negotiation between both modules. Thus, the PDM takes as an input the data of the profile requested by the negotiation module, the meteorological data to determine the production, the storage situations, etc.

As an output, the PDM must send more or less a similar profile to the one received by the NM.

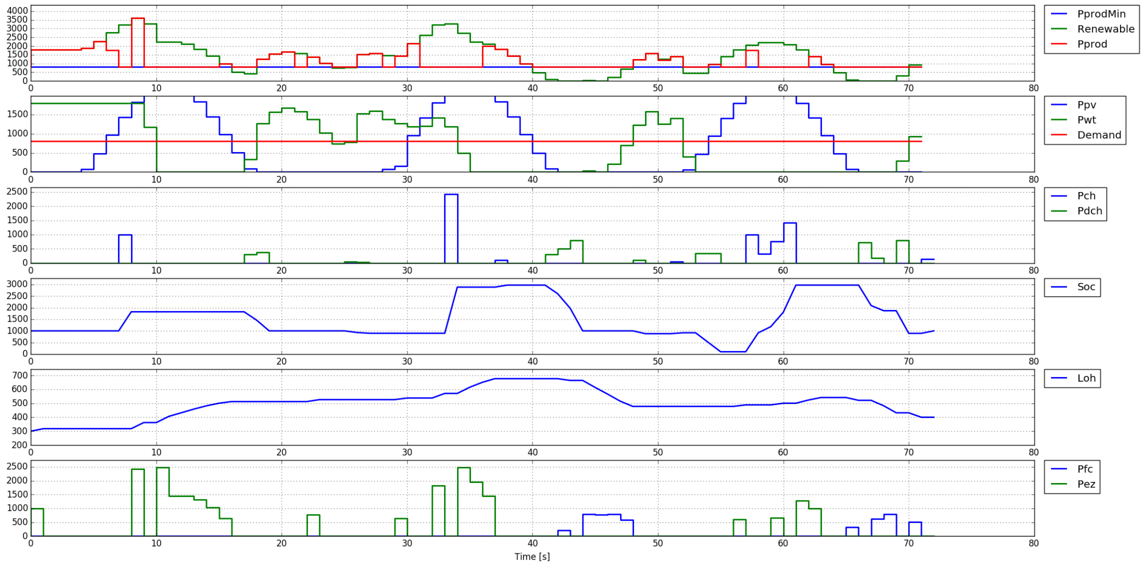

Figure 5: Maximum Power Profile management

To make this possible, some modifications are set for the basic linear program obtained and a new objective function and new constraints are added. To simplify it, the new variables added are explained in Table 4.

Table 4: Notations

Variable	**Description**
rf	Relaxation factor

6.3.1 Objective function

The objective function consists in maximizing the power profile obtained from the source commitment *Pprod* in order to address to the data center load. The problem is thus mathematically translated to:

$$\text{maximize} \quad \sum_{k=0}^{K-1} Pprod_k \tag{37}$$

6.3.2 Added constraints

As in the two previous cases, considering common sense usage rules turns Equation (11) into Equation (35). The constraint (33) is added in order to maximize the hydrogen level at the end of the period of simulation so the storage system is able to handle the next period. In this stage of the negotiation, in order to satisfy the profile requested by NM, a new constraint is added to the linear program as defined in Equation (38). Therefore, we introduce a rf provided by the negotiation module and enable the power produced $Pprod_k$ in each time step k to be inside an interval $[(1 - rf) \times Pload_k, (rf + 1) \times Pload_k]$.

$$(1 - rf)Pload_k \leq Pprod_k \leq (rf + 1)Pload_k \tag{38}$$

The feasibility of the linear program depends on the rf value:

- if $rf = 0$ it means that the profile generated must the same as the one provided by the NM
- if $rf = 1$ it means that the profile could be entirely different from the one provided

If rf is too small or equal to zero, the linear program is not always able to find a solution depending on the storage level. In this case, we propose to increase the relax factor received from NM.

6.3.3 Obtained model

The linear program able to produce a profile that matches with a given one from the negotiation module using the storage system is then written as mentioned in the appendix D.

6.3.4 Results

Results presented in Figure 6 are obtained by applying this linear program. The production *Pprod* is completely similar to the demand (here the demand represents the power profile received from the negotiation module) as the relax factor is equal to 0. The same power architecture is used as in the previous section. The load is variable between 500 kW and 2 MW in this case in order to see better variation of the profile. The battery assures the smoothing of the day/night alternation and come back to the same level each 24h. At the end of the horizon, starting from the hour 64, one can see an underproduction, the battery and the fuel cell are then working in order to reach the demand. Nevertheless, the constraint 33 is maintained and level of hydrogen at the end of the horizon is equal to the target fixed 300 kg

If one considers a $rf = 0.5$, the results of the MILP are as showed in the figure 7. As we can see it, the profile generated is different from the provided one and respects the constraint given in Eq 38. If we compare Figures 6 and Figure 7, the main difference is in the storage behaviour. In the second case, one can see that the storage state of the battery is not varying and stay almost constant all over the horizon while the hydrogen level is varying and is bigger than the target fixed at the end of the horizon $LOH_K = 400\,kg$. This is due to the freedom given by the relax factor.

6.4 Source commitment

6.4.1 Objective function

The objective function is to maximize long-term stocks by setting a target level hydrogen to reach at each end of horizon. Target stocks are set by the previsions of renewable energy production and by the capabilities of the components. The problem is thus mathematically translated by minimizing the difference in energy between the hydrogen level calculated at the end of the $\mathcal{H}$ horizon (LOH_K) and a hydrogen target level ($LOHtarget_D$) which is equivalent to maximize the level of hydrogen LOH_K at the end of the horizon $\mathcal{H}$.

The objective function is defined as:

$$\text{minimize} \quad LOHtarget_D - LOH_K \tag{39}$$

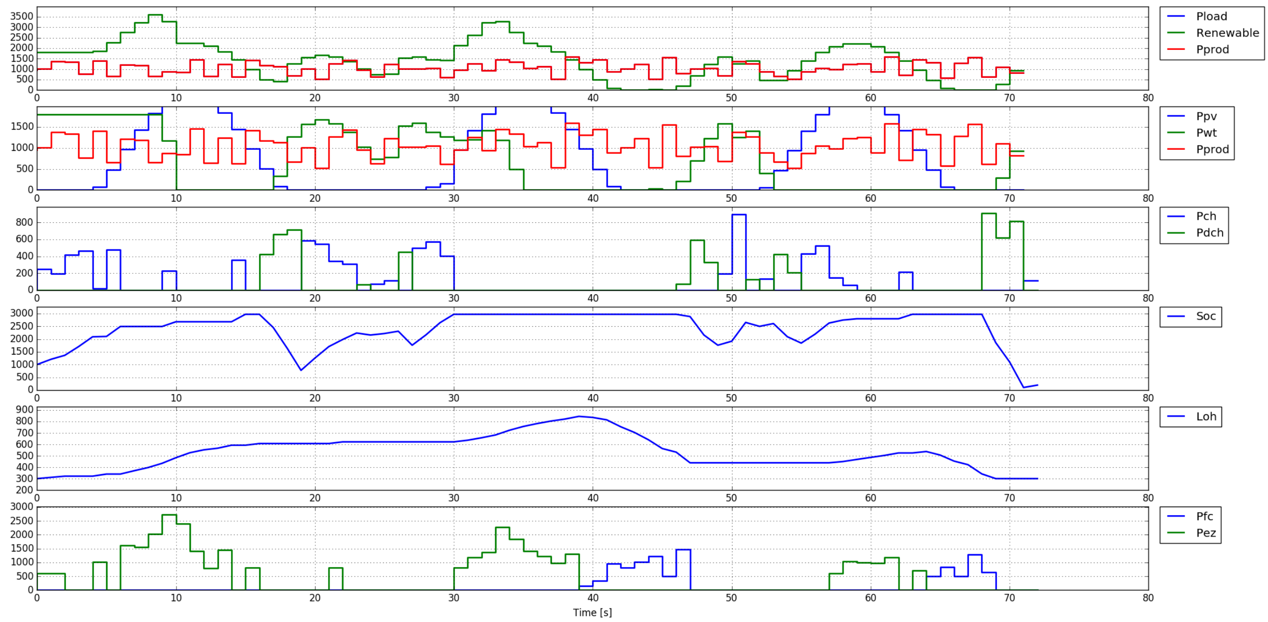

Figure 6: Management of the resources to match with a requested profile with $rf = 0$

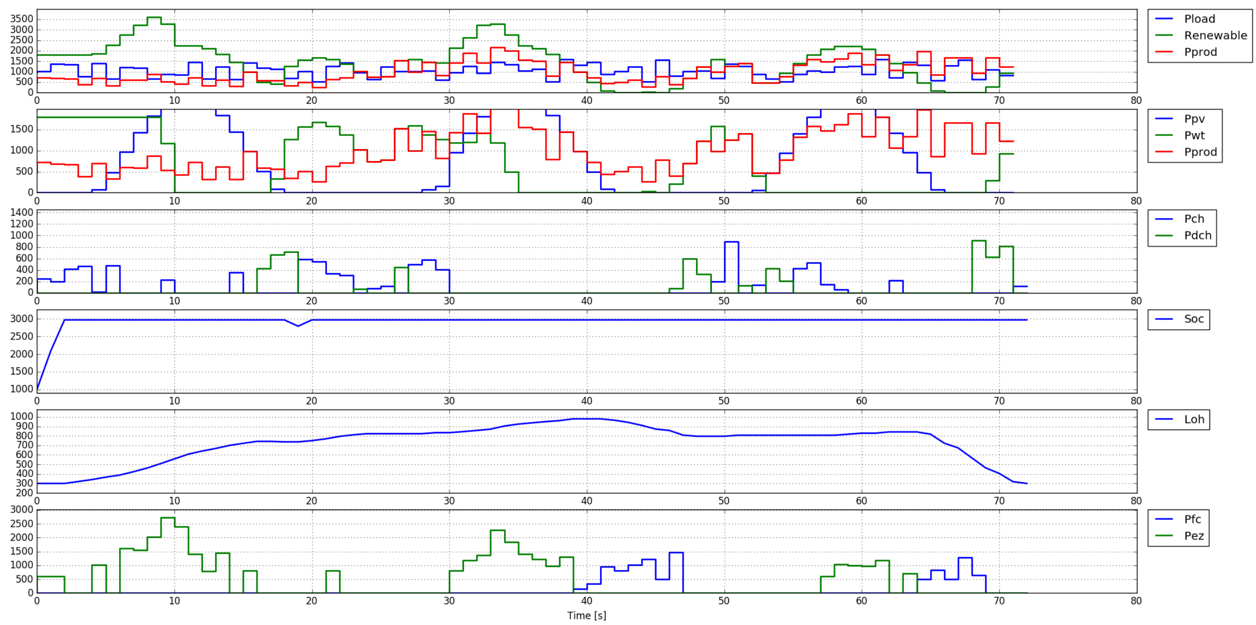

Figure 7: Management of the resources to match with a requested profile with $rf = 0.5$

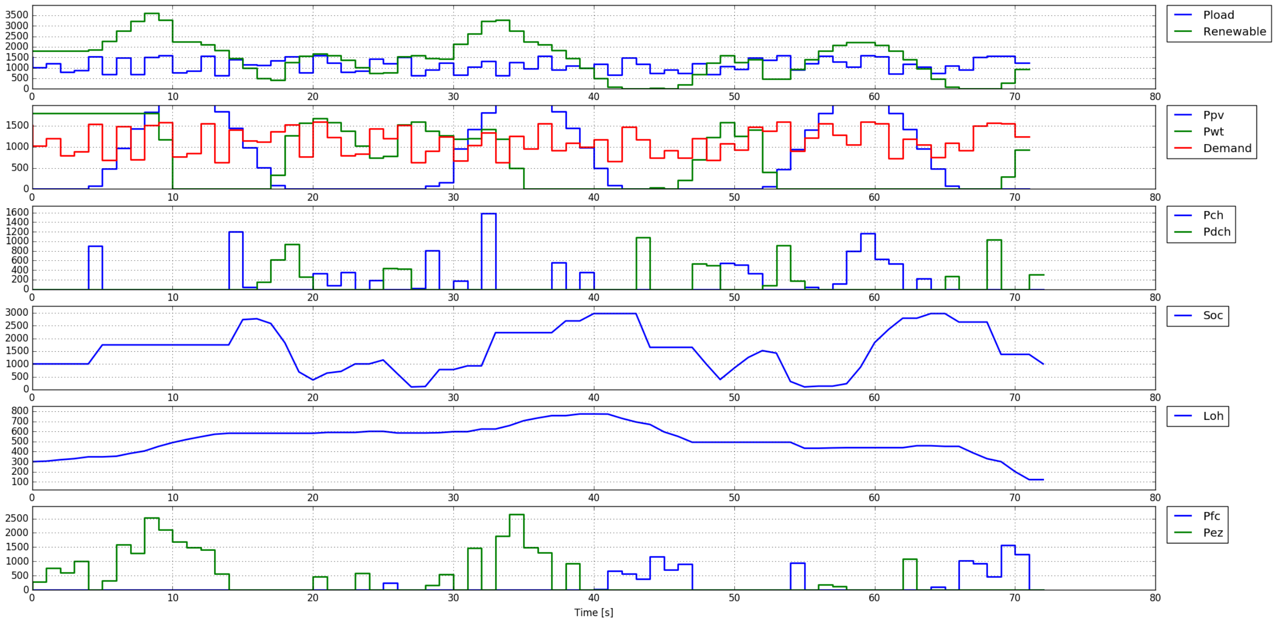

Figure 8: Source commitment results

6.4.2 Obtained model

The linear program obtained for the source commitment is defined, $\forall k \in [\![0, K-1]\!]$ for all constraints except $k \in [\![0, K]\!]$ for constraints containing variables SOC_k, LOH_k, Qez_k, Qfc_k, Qez'_k and Qfc'_k as mentioned in the appendix A.

6.4.3 Results

The figure 8 shows the management of the different resources following the constraints explained in the previous sections. The power profile agreed on after the negotiation will be designed with the best assignment of the sources. One can also see that all the constraints are respected, especially for the mutual exclusion between hydrogen and battery. Finally, we notice that the level of hydrogen is decreasing at the end of the horizon $\mathcal{H} = 72\,h$ as well ass the level of the battery because of the lack of renewable production.

6.5 Summary of the results

the results above suggest several interesting observations:

- The sizing of the electrical sources is very important as well as the values of the initial state of storage. They allow a good running of the programs. Otherwise, the management tool can provide an unfeasible model.

- The MILP that Match with a given profile depends extremely of the relax factor provided from the negotiation module. Sometimes, given the storage state at the moment of the negotiation, the management tool provide an unfeasible model and is not capable to answer to the demand. The negotiation take action here and send a second profile with a different relax factor

- The analysis of the curves of the MILP "Match Profile" shows an average gap between the curves Pprod and Pload as shown in following table:

rf	$\sum Pprod$	$\sum Pload$	$\overline{gap}$	Period
0	63820.0 kW	63820.0 kW	0.00	72 h
0.4	65532.0 kW	63820.0 kW	23.78	72 h
0.8	67922.0 kW	63820.0 kW	56.98	72 h
1	68993.4 kW	63820.0 kW	71.85	72 h

- The results of the table 6.5 are obtained after an execution of the MILP during 72 hours while respecting the constraint 38. This constraint force the program to always be in the interval given.

- The execution time of the algorithms is at the scale of seconds which is compatible with the negotiation process as it's a synchronous negotiation.

- The PDM is an efficient management tool of all energy sources (wind turbine, photovoltaics, batteries, fuel cell, electrolyzers) that is able to provide data center demand with 100% renewable energy

7 Conclusion

In this paper, we presented (1) an analysis of the main trade offs involved in powering data centers with hybrid renewable energy system and the ANR DATAZERO project that aims to completely provide a data center with only renewable energy (2) a model of HRES composed of wind turbines, photovoltaic panels, batteries and hydrogen system (3) the problem statement defined by powering the demand of the data center with only renewable energy and the constraint satisfaction problem due to it (4) the linearization of the constraints in order to get a convenient usage of the sources and the mixed linear program which is used in the PDM (5) the power decision module which is a management tool able to manage a hybrid renewable energy system presenting four optimization problems depending on the stage of the negotiation. Additional constraints are also written to allow us to find appropriate solutions. These problems have been illustrated by several simulation. We show that our optimal models are convenient to address the power commitment of an 100% renewable energy data center, since the resolution is obtained within few seconds. As future works, we plan to consider the ageing of power sources in order to play maintenance scenarios similar to the real life one. For instance, one can manage in various manner one wind turbine or one battery depending on its degradation level so as to improve the sustainability of the power platform.

Acknowledgment

This work was supported in part by the ANR DATAZERO (contract "ANR-15-CE25-0012") project and by the EIPHI Graduate school (contract "ANR-17-EURE-0002").

References

[1] Baris Aksanli, Jagannathan Venkatesh, Liuyi Zhang, and Tajana Rosing. Utilizing green energy prediction to schedule mixed batch and service jobs in data centers. In *Proceedings of the 4th Workshop on Power-Aware Computing and Systems*, page 5. ACM, 2011.

[2] Apple. Apple facilities, environmental footprint report. *Apple and the Environment*, 2013.

[3] Martin Arlitt, Cullen Bash, Sergey Blagodurov, Yuan Chen, Tom Christian, Daniel Gmach, Chris Hyser, Niru Kumari, Zhenhua Liu, Manish Marwah, et al. Towards the design and operation of net-zero energy data centers. In *Thermal and Thermomechanical Phenomena in Electronic Systems (ITherm), 2012 13th IEEE Intersociety Conference on*, pages 552–561. IEEE, 2012.

[4] Stéphane Caux, Gustavo Rostirolla, and Patricia Stolf. Smart Datacenter Electrical Load Model for Renewable Sources Management. In *International Conference on Renewable Energies and Power Quality (ICREPQ), Salamanca, Spain, 21/03/2018-23/03/2018*, volume 16, page (on line), http://www.icrepq.com, 2018. European Association for the Development of Renewable Energies, Environment and Power Quality.

[5] Gary Cook, J Lee, T Tsai, A Kong, J Deans, B Johnson, and E Jardim. Clicking clean: Who is winning the race to build a green internet? *Greenpeace Inc., Washington, DC*, 2017.

[6] ANR DATAZERO project, 2015–2019. http://datazero.org.

[7] Wei Deng, Fangming Liu, Hai Jin, and Xiaofei Liao. Online control of datacenter power supply under uncertain demand and renewable energy. In *Communications (ICC), 2013 IEEE International Conference on*, pages 4228–4232. IEEE, 2013.

[8] Íñigo Goiri, William Katsak, Kien Le, Thu D. Nguyen, and Ricardo Bianchini. Parasol and greenswitch: Managing datacenters powered by renewable energy. *SIGARCH Comput. Archit. News*, 41(1):51–64, March 2013.

[9] Íñigo Goiri, Ryan Beauchea, Kien Le, Thu D Nguyen, Md E Haque, Jordi Guitart, Jordi Torres, and Ricardo Bianchini. Greenslot: scheduling energy consumption in green datacenters. In *High Performance Computing, Networking, Storage and Analysis (SC), 2011 International Conference for*, pages 1–11. IEEE, 2011.

[10] Íñigo Goiri, Md E Haque, Kien Le, Ryan Beauchea, Thu D Nguyen, Jordi Guitart, Jordi Torres, and Ricardo Bianchini. Matching renewable energy supply and demand in green datacenters. *Ad Hoc Networks*, 25:520–534, 2015.

[11] Sriram Govindan, Anand Sivasubramaniam, and Bhuvan Urgaonkar. Benefits and limitations of tapping into stored energy for datacenters. In *Computer Architecture (ISCA), 2011 38th Annual International Symposium on*, pages 341–351. IEEE, 2011.

[12] Sriram Govindan, Di Wang, Anand Sivasubramaniam, and Bhuvan Urgaonkar. Leveraging stored energy for handling power emergencies in aggressively provisioned datacenters. In *ACM SIGARCH Computer Architecture News*, volume 40(1), pages 75–86. ACM, 2012.

[13] Inc. Gurobi Optimization. Gurobi optimizer reference manual, 2016.

[14] Daniel Hackenberg, Robert Schöne, Thomas Ilsche, Daniel Molka, Joseph Schuchart, and Robin Geyer. An energy efficiency feature survey of the intel haswell processor. In *International Parallel and Distributed Processing Symposium Workshop (IPDPSW)*, pages 896–904. IEEE, 2015.

[15] Marwa Haddad, Jean-Marc Nicod, and Marie-Cécile Péra. data-center supply-refueling station synergy. In *Vehicle Power and Propulsion Conference (VPPC 2017)*, pages 1 – 6, Belfort, dec 2017. IEEE.

[16] Johannes Hofmann, Dietmar Fey, Jan Eitzinger, Georg Hager, and Gerhard Wellein. Analysis of intel's haswell microarchitecture using the ecm model and microbenchmarks. In *International Conference on Architecture of Computing Systems*, pages 210–222. Springer, 2016.

[17] A. Kassab, J. M. Nicod, L. Philippe, and V. Rehn-Sonigo. Scheduling independent tasks in parallel under power constraints. In *46th International Conference on Parallel Processing (ICPP)*, pages 543–552, Bristol, UK, aug 2017.

[18] Randy H Katz. Tech titans building boom. *IEEE spectrum*, 46(2):40–54, 2009.

[19] Tarandeep Kaur and Inderveer Chana. Energy efficiency techniques in cloud computing: A survey and taxonomy. *ACM Computing Surveys (CSUR)*, 48(2):22, 2015.

[20] Vasileios Kontorinis, Liuyi Eric Zhang, Baris Aksanli, Jack Sampson, Houman Homayoun, Eddie Pettis, Dean M Tullsen, and Tajana Simunic Rosing. Managing distributed ups energy for effective power capping in data centers. In *Computer Architecture (ISCA), 2012 39th Annual International Symposium on*, pages 488–499. IEEE, 2012.

[21] Jonathan Koomey. Growth in data center electricity use 2005 to 2010. *A report by Analytical Press, completed at the request of The New York Times*, 9, 2011.

[22] Hongtao Lei, Tao Zhang, Yajie Liu, Yabing Zha, and Xiaomin Zhu. Sgeess: Smart green energy-efficient scheduling strategy with dynamic electricity price for data center. *Journal of Systems and Software*, 108:23–38, 2015.

[23] Chao Li, Rui Wang, Tao Li, Depei Qian, and Jingling Yuan. Managing green datacenters powered by hybrid renewable energy systems. In *The 11th International Conference on Autonomic Computing*, pages 261–272. USENIX, 2014.

[24] Jie Li, Zuyi Li, Kui Ren, and Xue Liu. Towards optimal electric demand management for internet data centers. *IEEE Transactions on Smart Grid*, 3(1):183–192, 2012.

[25] Zhenhua Liu, Yuan Chen, Cullen Bash, Adam Wierman, Daniel Gmach, Zhikui Wang, Manish Marwah, and Chris Hyser. Renewable and cooling aware workload management for sustainable data centers. In *ACM SIGMETRICS Performance Evaluation Review*, volume 40(1), pages 175–186. ACM, 2012.

[26] Rich Miller. Huge solar array will support nj data center. *datacenterknowledge*, 2011. http://www.datacenterknowledge.com/archives/2011/06/14/huge-solar-array-will-support-nj-data-center/.

[27] Anne-Cecile Orgerie, Marcos Dias de Assuncao, and Laurent Lefevre. A survey on techniques for improving the energy efficiency of large-scale distributed systems. *ACM Comput. Surv.*, 46(4):47:1–47:31, March 2014.

[28] Eduard Oró, Victor Depoorter, Albert Garcia, and Jaume Salom. Energy efficiency and renewable energy integration in data centres. strategies and modelling review. *Renewable and Sustainable Energy Reviews*, 42:429–445, 2015.

[29] Enida Sheme, Patricia Stolf, Georges Da Costa, Jean-Marc Pierson, and Neki Frashëri. Efficient energy sources scheduling in green powered datacenters: A cloudsim implementation. *NESUS workshop*, 2016.

[30] P. Stolf, D. Borgetto, and M. Aubert. Host management policy for energy efficient dynamic allocation. In *2016 Seventh International Green and Sustainable Computing Conference (IGSC)*, pages 1–7, Hangzhou, China, Nov 2016.

[31] P Thibodeau. Wind power data center project planned in urban area. *ComputerWorld, Apr*, 2008.

[32] Mueen Uddin and Azizah Abdul Rahman. Techniques to implement in green data centres to achieve energy efficiency and reduce global warming effects. *International Journal of Global Warming*, 3(4):372–389, 2011.

[33] Mueen Uddin and Azizah Abdul Rahman. Energy efficiency and low carbon enabler green it framework for data centers considering green metrics. *Renewable and Sustainable Energy Reviews*, 16(6):4078–4094, 2012.

[34] Mueen Uddin, Azizah Abdul Rahman, and Asadullah Shah. Criteria to select energy efficiency metrics to measure performance of data centre. *International Journal of Energy Technology and Policy*, 8(3-6):224–237, 2012.

[35] Mueen Uddin, Asadullah Shah, and Raed Alsaqour. Implementation of virtualization in data centers to increase proficiency and performance. *Journal of Theoretical & Applied Information Technology*, 53(2), 2013.

[36] Rahul Urgaonkar, Bhuvan Urgaonkar, Michael J Neely, and Anand Sivasubramaniam. Optimal power cost management using stored energy in data centers. In *Proceedings of the ACM SIGMETRICS joint international conference on Measurement and modeling of computer systems*, pages 221–232. ACM, 2011.

[37] Di Wang, Chuangang Ren, Anand Sivasubramaniam, Bhuvan Urgaonkar, and Hosam Fathy. Energy storage in datacenters: what, where, and how much? In *ACM SIGMETRICS Performance Evaluation Review*, volume 40(1), pages 187–198. ACM, 2012.

Appendices

A Sources commitment

The obtained model used for the source commitment is defined as follow:

$$
\begin{cases}
\begin{array}{rcl}
 & & \text{minimize} \quad LOHtarget_D - LOH_K \\
s.t.: & & \\
Pload_k & \leq & Pwt_k + Ppv_k + (Pfc_k + Pdch_k)\eta_{inv} \\
 & & -(Pez_k + Pch_k)\eta_{inv} \\
SOC_k & = & SOC_{k-1}(1-\sigma) + Pch_{k-1}\Delta t \times \eta_{ch} \\
 & & -Pdch_{k-1}\Delta t/\eta_{dch} \\
Pez_k & = & HHVh_2 \times Qez_k/\eta_{ez}/\Delta t \\
Pfc_k & = & LHVh_2 \times Qfc_k \times \eta_{fc}/\Delta t \\
LOH_k & = & LOH_{k-1} + Qez_{k-1} - Qfc_{k-1}/\eta_{tank} \\
Pch_k & \leq & x_k \times Pchmax \\
Pch_k & \geq & 0 \\
Pch_k & \leq & x_k \times Pchmax \\
Pch_k & \leq & Pch'_k \\
Pch_k & \geq & Pch'_k - (1-x_k)Pchmax \\
Pdch_k & \leq & (1-x_k) \times Pdchmax \\
Pdch_k & \geq & 0 \\
Pdch_k & \leq & (1-x_k)Pdchmax \\
Pdch_k & \leq & Pdch'_k \\
Pdch_k & \geq & Pdch'_k - x_k Pdchmax \\
Pez_k & \leq & Pez'_k \\
Pez_k & \geq & 0 \\
Pez_k & \leq & y_k \times Pezmax \\
Pez_k & \geq & Pez'_k - (1-y_k)Pezmax \\
0 & \leq & Pez'_k \leq Pezmax \\
Pez_k & \geq & y_k \times Pezmin \\
Qez_k & \leq & Qez'_k \\
Qez_k & \geq & 0 \\
Qez_k & \leq & z_k \times Qezmax \\
Qez_k & \geq & Qez'_k - (1-z_k)Qezmax \\
0 & \leq & Qez'_k \leq Qezmax \\
Qfc_k & \leq & Qfc'_k \\
Qfc_k & \geq & 0 \\
Qfc_k & \leq & (1-z_k) \times Qfcmax \\
Qfc_k & \geq & Qfc'_k - z_k \times Qfcmax \\
0 & \leq & Qfc'_k \leq Qfcmax \\
u_k & \leq & x_k \\
u_k & \leq & y_k \\
0 & \leq & 1 - x_k - y_k + u \\
u_k & \geq & 0 \\
v_k & \leq & x_k \\
v_k & \leq & z_k \\
0 & \leq & 1 - x_k - z_k + v \\
v_k & \geq & 0
\end{array}
\end{cases}
$$

B Providing a constant power profile

The obtained model used to provide a constant power profile as a first proposition for the negotiation is:

$$
\left\{
\begin{array}{rcl}
& & \text{maximize } Pprod \\
s.t.: & & \\
Pprod & \leq & Pwt_k + Ppv_k + (Pfc_k + Pdch_k)\eta_{inv} \\
& & -(Pez_k + Pch_k)\eta_{inv} \\
SOC_k & = & SOC_{k-1}(1-\sigma) + \eta_{ch} Pch_{k-1}\Delta t \\
& & -Pdch_{k-1}\Delta t/\eta_{dch} \\
LOH_K & \geq & LOHtarget_D \\
Pload_k & \leq & Pwt_k + Ppv_k + (Pfc_k + Pdch_k)\eta_{inv} \\
& & -(Pez_k + Pch_k)\eta_{inv} \\
SOC_k & = & SOC_{k-1}(1-\sigma) + Pch_{k-1}\Delta t \times \eta_{ch} \\
& & -Pdch_{k-1}\Delta t/\eta_{dch} \\
Pez_k & = & HHVh_2 \times Qez_k/\eta_{ez}/\Delta t \\
Pfc_k & = & LHVh_2 \times Qfc_k \times \eta_{fc}/\Delta t \\
LOH_k & = & LOH_{k-1} + Qez_{k-1} - Qfc_{k-1}/\eta_{tank} \\
Pch_k & \leq & x_k \times Pchmax \\
Pch_k & \geq & 0 \\
Pch_k & \leq & x_k \times Pchmax \\
Pch_k & \leq & Pch'_k \\
Pch_k & \geq & Pch'_k - (1-x_k)Pchmax \\
Pdch_k & \leq & (1-x_k) \times Pdchmax \\
Pdch_k & \geq & 0 \\
Pdch_k & \leq & (1-x_k)Pdchmax \\
Pdch_k & \leq & Pdch'_k \\
Pdch_k & \geq & Pdch'_k - x_k Pdchmax \\
Pez_k & \leq & Pez'_k \\
Pez_k & \geq & 0 \\
Pez_k & \leq & y_k \times Pezmax \\
Pez_k & \geq & Pez'_k - (1-y_k)Pezmax \\
0 & \leq & Pez'_k \leq Pezmax \\
Pez_k & \geq & y_k \times Pezmin \\
Qez_k & \leq & Qez'_k \\
Qez_k & \geq & 0 \\
Qez_k & \leq & z_k \times Qezmax \\
Qez_k & \geq & Qez'_k - (1-z_k)Qezmax \\
0 & \leq & Qez'_k \leq Qezmax \\
Qfc_k & \leq & Qfc'_k \\
Qfc_k & \geq & 0 \\
Qfc_k & \leq & (1-z_k) \times Qfcmax \\
Qfc_k & \geq & Qfc'_k - z_k \times Qfcmax \\
0 & \leq & Qfc'_k \leq Qfcmax \\
u_k & \leq & x_k \\
u_k & \leq & y_k \\
0 & \leq & 1 - x_k - y_k + u \\
u_k & \geq & 0 \\
v_k & \leq & x_k \\
v_k & \leq & z_k \\
0 & \leq & 1 - x_k - z_k + v \\
v_k & \geq & 0
\end{array}
\right.
\qquad
\left\{
\begin{array}{ll}
Bounds: & \\
\forall k \in [\![0, K-1]\!] & Pfc_k \leq Pfcmax \\
\forall k \in [\![0, K-1]\!] & Pez_k \geq Pezmin \\
\forall k \in [\![0, K]\!] & SOCmin \leq SOC_k \leq SOCmax \\
\forall k \in [\![0, K]\!] & 0 \leq LOH_k \leq LOH_{max} \\
\forall k \in [\![0, K-1]\!] & Pch_k, Pdch_k, Pez_k, Pch'_k, Pdch'_k, Pez'_k \geq 0 \\
\forall k \in [\![0, K-1]\!] & Qez_k, Qfc_k, Qez'_k, Qfc'_k \geq 0 \\
\forall k \in [\![0, K-1]\!] & x_k, y_k, z_k \in \{0, 1\}
\end{array}
\right.
$$

C Providing a non constant power profile

The obtained model used to provide a non constant power profile as a proposition for the negotiation is:

$$
\begin{cases}
Bounds: & \\
\forall k \in [\![0, K-1]\!] & Pfc_k \leq Pfcmax \\
\forall k \in [\![0, K-1]\!] & Pez_k \geq Pezmin \\
\forall k \in [\![0, K]\!] & SOCmin \leq SOC_k \leq SOCmax \\
\forall k \in [\![0, K]\!] & 0 \leq LOH_k \leq LOH_{max} \\
\forall k \in [\![0, K-1]\!] & Pch_k, Pdch_k, Pez_k, Pch'_k, Pdch'_k, Pez'_k \geq 0 \\
\forall k \in [\![0, K-1]\!] & Qez_k, Qfc_k, Qez'_k, Qfc'_k \geq 0 \\
\forall k \in [\![0, K-1]\!] & x_k, y_k, z_k \in \{0, 1\}
\end{cases}
$$

$$
\begin{cases}
 & & \text{maximize } \sum_{k=0}^{K-1} Pprod_k \\
s.t.: & & \\
Pprod_k & \leq & Pwt_k + Ppv_k + (Pfc_k + Pdch_k)\eta_{inv} \\
 & & -(Pez_k + Pch_k)\eta_{inv} \\
SOC_k & = & SOC_{k-1}(1-\sigma) + \eta_{ch} Pch_{k-1}\Delta t \\
 & & -Pdch_{k-1}\Delta t/\eta_{dch} \\
LOH_K & \geq & LOHtarget_D \\
Pprod_k & \geq & Pprodmin \\
Pez_k & = & HHVh_2 \times Qez_k/\eta_{ez}/\Delta t \\
Pfc_k & = & LHVh_2 \times Qfc_k \times \eta_{fc}/\Delta t \\
LOH_k & = & LOH_{k-1} + Qez_{k-1} - Qfc_{k-1}/\eta_{tank} \\
Pch_k & \leq & x_k \times Pchmax \\
Pch_k & \geq & 0 \\
Pch_k & \leq & x_k \times Pchmax \\
Pch_k & \leq & Pch'_k \\
Pch_k & \geq & Pch'_k - (1-x_k)Pchmax \\
Pdch_k & \leq & (1-x_k) \times Pdchmax \\
Pdch_k & \geq & 0 \\
Pdch_k & \leq & (1-x_k)Pdchmax \\
Pdch_k & \leq & Pdch'_k \\
Pdch_k & \geq & Pdch'_k - x_k Pdchmax \\
Pez_k & \leq & Pez'_k \\
Pez_k & \geq & 0 \\
Pez_k & \leq & y_k \times Pezmax \\
Pez_k & \geq & Pez'_k - (1-y_k)Pezmax \\
0 & \leq & Pez'_k \leq Pezmax \\
Pez_k & \geq & y_k \times Pezmin \\
Qez_k & \leq & Qez'_k \\
Qez_k & \geq & 0 \\
Qez_k & \leq & z_k \times Qezmax \\
Qez_k & \geq & Qez'_k - (1-z_k)Qezmax \\
0 & \leq & Qez'_k \leq Qezmax \\
Qfc_k & \leq & Qfc'_k \\
Qfc_k & \geq & 0 \\
Qfc_k & \leq & (1-z_k) \times Qfcmax \\
Qfc_k & \geq & Qfc'_k - z_k \times Qfcmax \\
0 & \leq & Qfc'_k \leq Qfcmax \\
u_k & \leq & x_k \\
u_k & \leq & y_k \\
0 & \leq & 1 - x_k - y_k + u \\
u_k & \geq & 0 \\
v_k & \leq & x_k \\
v_k & \leq & z_k \\
0 & \leq & 1 - x_k - z_k + v \\
v_k & \geq & 0
\end{cases}
$$

D Matching with a requested profile

The obtained model used to provide a power profile that can match with a power profile received from the negotiation is:

$$
\begin{cases}
 & & \text{maximize} \quad \sum_{k=0}^{K-1} \; Pprod_k \\
s.t.: & & \\
Pprod_k & \leq & Pwt_k + Ppv_k + (Pfc_k + Pdch_k)\eta_{inv} \\
 & & -(Pez_k + Pch_k)\eta_{inv} \\
SOC_k & = & SOC_{k-1}(1-\sigma) + \eta_{ch} Pch_{k-1}\Delta t \\
 & & -Pdch_{k-1}\Delta t/\eta_{dch} \\
LOH_K & \geq & LOHtarget_D \\
Pprod_k & \geq & (1-rf) \times Load_k \\
 & & \leq (rf+1) \times Load_k \\
Pez_k & = & HHVh_2 \times Qez_k/\eta_{ez}/\Delta t \\
Pfc_k & = & LHVh_2 \times Qfc_k \times \eta_{fc}/\Delta t \\
LOH_k & = & LOH_{k-1} + Qez_{k-1} - Qfc_{k-1}/\eta_{tank} \\
Pch_k & \leq & x_k \times Pchmax \\
Pch_k & \geq & 0 \\
Pch_k & \leq & x_k \times Pchmax \\
Pch_k & \leq & Pch'_k \\
Pch_k & \geq & Pch'_k - (1-x_k)Pchmax \\
Pdch_k & \leq & (1-x_k) \times Pchmax \\
Pdch_k & \geq & 0 \\
Pdch_k & \leq & (1-x_k)Pdchmax \\
Pdch_k & \leq & Pdch'_k \\
Pdch_k & \geq & Pdch'_k - x_k Pdchmax \\
Pez_k & \leq & Pez'_k \\
Pez_k & \geq & 0 \\
Pez_k & \leq & y_k \times Pezmax \\
Pez_k & \geq & Pez'_k - (1-y_k)Pezmax \\
0 & \leq & Pez'_k \leq Pezmax \\
Pez_k & \geq & y_k \times Pezmin \\
Qez_k & \leq & Qez'_k \\
Qez_k & \geq & 0 \\
Qez_k & \leq & z_k \times Qezmax \\
Qez_k & \geq & Qez'_k - (1-z_k)Qezmax \\
0 & \leq & Qez'_k \leq Qezmax \\
Qfc_k & \leq & Qfc'_k \\
Qfc_k & \geq & 0 \\
Qfc_k & \leq & (1-z_k) \times Qfcmax \\
Qfc_k & \geq & Qfc'_k - z_k \times Qfcmax \\
0 & \leq & Qfc'_k \leq Qfcmax \\
u_k & \leq & x_k \\
u_k & \leq & y_k \\
0 & \leq & 1 - x_k - y_k + u \\
u_k & \geq & 0 \\
v_k & \leq & x_k \\
v_k & \leq & z_k \\
0 & \leq & 1 - x_k - z_k + v \\
v_k & \geq & 0
\end{cases}
\qquad
\begin{cases}
Bounds: & \\
\forall k \in [\![0, K-1]\!] & Pfc_k \leq Pfcmax \\
\forall k \in [\![0, K-1]\!] & Pez_k \geq Pezmin \\
\forall k \in [\![0, K]\!] & SOCmin \leq SOC_k \leq SOCmax \\
\forall k \in [\![0, K]\!] & 0 \leq LOH_k \leq LOH_{max} \\
\forall k \in [\![0, K-1]\!] & Pch_k, Pdch_k, Pez_k, Pch'_k, Pdch'_k, Pez'_k \geq 0 \\
\forall k \in [\![0, K-1]\!] & Qez_k, Qfc_k, Qez'_k, Qfc'_k \geq 0 \\
\forall k \in [\![0, K-1]\!] & x_k, y_k, z_k \in \{0, 1\}
\end{cases}
$$

FEMTO-ST INSTITUTE, headquarters
15B Avenue des Montboucons - F-25030 Besançon Cedex France
Tel: (33 3) 63 08 24 00 – e-mail: contact@femto-st.fr

FEMTO-ST — AS2M: TEMIS, 24 rue Alain Savary, F-25000 Besançon France
FEMTO-ST — DISC: UFR Sciences - Route de Gray - F-25030 Besançon cedex France
FEMTO-ST — ENERGIE: Parc Technologique, 2 Av. Jean Moulin, Rue des entrepreneurs, F-90000 Belfort France
FEMTO-ST — MEC'APPLI: 24, chemin de l'épitaphe - F-25000 Besançon France
FEMTO-ST — MN2S: 15B Avenue des Montboucons - F-25030 Besançon cedex France
FEMTO-ST — OPTIQUE: 15B Avenue des Montboucons - F-25030 Besançon cedex France
FEMTO-ST — TEMPS-FREQUENCE: 26, Chemin de l'Epitaphe - F-25030 Besançon cedex France

http://www.femto-st.fr